DOI 10.59887/2073-6673.2024.17(3)-3

UDC 551.46.08

© *V. A. Glukhov**[1], *Yu. A. Goldin*[1], *O. V. Glitko*[1], *D. I. Glukhovets*[1,2], *M. A. Rodionov*[1], 2024
© Translation from Russian: *V. A. Glukhov*, 2024

[1]Shirshov Institute of Oceanology, Russian Academy of Sciences, 117997, Nakhimovsky pr., 36, Moscow, Russia
[2]Moscow Institute of Physics and Technology (National Research University), 141701, Institutskiy per., 9, Dolgoprudny, Moscow Region, Russia
*vl.glukhov@inbox.ru

A COMPARISON OF THE INFORMATION CONTENT OF ORTHOGONALLY POLARIZED COMPONENTS OF LIDAR ECHO SIGNAL FOR EVALUATING HYDROOPTICAL CHARACTERISTICS OF THE NEAR-SURFACE LAYER

Received 29.05.2024, Revised 26.07.2024, Accepted 10.09.2024

Abstract

A series of lidar measurements were conducted at stations with a homogeneous vertical distribution of hydrooptical characteristics in the near-surface layer using a two-channel shipborne polarization lidar PLD-1. Lidar sounding was accompanied by synchronous contact measurements of a number of hydrooptical characteristics. A large dataset of measurement data was obtained in waters where hydrooptical characteristics varied widely. As a result of the statistical processing of these data, regression relationships were obtained linking the seawater beam attenuation coefficient c, absorption coefficient a, and diffuse attenuation coefficient K_d to the lidar attenuation coefficients of the co- and cross-polarized components. In most cases, a linear relationship between hydrooptical characteristics and the lidar attenuation coefficients of the polarized components is observed. These relationships are characterized by high values of the coefficient of determination — from 0.8 to 0.95. An exception is the relationship between the seawater beam attenuation coefficient c and the lidar attenuation coefficient of the cross-polarized component, where a second-degree polynomial is used to describe this relationship (coefficient of determination is 0.88). Data on the hydrooptical characteristics obtained using the cross-polarized component of the lidar echo signal mostly duplicate the data of the co-polarized component. However, the use of a two-channel optical receiving system increases the reliability and accuracy of the obtained data and provides the possibility of controlling the homogeneity of the underwater section of the sounding path.

Keywords: marine polarized lidar, hydrooptical characteristics, regression relationship

УДК 551.46.08

© *В. А. Глухов**[1], *Ю. А. Гольдин*[1], *О. В. Глитко*[1], *Д. И. Глуховец*[1,2], *М. А. Родионов*[1], 2024
© Перевод с русского: *В. А. Глухов*, 2024

[1]Институт океанологии им. П.П. Ширшова РАН, 117997, Нахимовский пр., д. 36, г. Москва, Россия
[2]Московский физико-технический институт (национальный исследовательский университет), 141701, Институтский пер., 9, г. Долгопрудный, Московская область, Россия
*vl.glukhov@inbox.ru

СОПОСТАВЛЕНИЕ ИНФОРМАТИВНОСТИ ОРТОГОНАЛЬНО ПОЛЯРИЗОВАННЫХ КОМПОНЕНТ ЛИДАРНОГО ЭХО-СИГНАЛА ДЛЯ ОЦЕНКИ ГИДРООПТИЧЕСКИХ ХАРАКТЕРИСТИК ПРИПОВЕРХНОСТНОГО СЛОЯ

Статья поступила в редакцию 29.05.2024, после доработки 26.07.2024, принята в печать 10.09.2024

Аннотация

С использованием двухканального судового поляризационного лидара ПЛД-1 на станциях с однородным вертикальным распределением гидрооптических характеристик приповерхностного слоя выполнена серия лидарных измерений. Лидарное зондирование сопровождалось синхронными сопутствующими контактными из-

Ссылка для цитирования: *Глухов В.А.*, *Гольдин Ю.А.*, *Глитко О.В.*, *Глуховец Д.И.*, Родионов М.А. Сопоставление информативности ортогонально поляризованных компонент лидарного эхо-сигнала для оценки гидрооптических характеристик приповерхностного слоя // Фундаментальная и прикладная гидрофизика. 2024. Т. 17, № 3. С. 32–43. doi:10.59887/2073-6673.2024.17(3)-8
For citation: Glukhov V.A., Goldin Yu.A., Glitko O.V., Glukhovets D.I., Rodionov M.A. A Comparison of the Information Content of Orthogonally Polarized Components of Lidar Echo Signal for Evaluating Hydrooptical Characteristics of the Near-Surface Layer. *Fundamental and Applied Hydrophysics*. 2024;17(3):32–43. doi:10.59887/2073-6673.2024.17(3)-8

мерениями ряда гидрооптических характеристик. Получен большой массив данных измерений, выполненных в водах с гидрооптическими характеристиками, меняющимися в широких пределах. В результате статистической обработки этих данных получены регрессионные соотношения, связывающие показатель ослабления c, показатель поглощения a и показатель диффузного ослабления света K_d с показателями ослабления ко- и кросс-поляризованных компонент лидарного эхо-сигнала. В большинстве случаев наблюдается линейная связь гидрооптических характеристик с показателями ослабления поляризованных компонент лидарного эхо-сигнала. Эти связи характеризуются высокими значениями коэффициента детерминации — от 0,8 до 0,95. Исключение составляет связь показателя ослабления света c и показателя ослабления кросс-поляризованной компоненты лидарного эхо-сигнала, где для описания этой связи используется полином второй степени (коэффициент детерминации 0,88). Данные о гидрооптических характеристиках, полученные с использованием кросс-поляризованной компоненты лидарного эхо-сигнала, в основном дублируют данные ко-поляризованной компоненты. Однако использование двухканальной регистрирующей системы повышает надежность и достоверность получаемых данных и обеспечивает возможность контроля однородности подводного участка трассы зондирования.

Ключевые слова: морской поляризационный лидар, гидрооптические характеристики, регрессионные соотношения

1. Introduction

Marine profiling (radiometric) lidars, as well as high spectral resolution lidars (HSRL) equipped with a profiling channel, enable remote assessment of the hydrooptical characteristics of the near-surface layer of seawater [1–10]. This facilitates the study of spatial distributions of hydrooptical characteristics from moving vessels without the need for submersible, towed, or flow-through measurement systems.

The lidar echo signal contains information about the hydrooptical characteristics of seawater. Several approaches exist for developing methods to extract this information. One such approach involves configuring the sounding scheme so that a particular parameter of the lidar echo signal depends solely on one hydrooptical characteristic [2, 4, 11]. For example, with sufficiently large field-of-view angles of the receiving optical system of a shipborne lidar ($2\gamma \sim 15°–20°$), the lidar attenuation coefficient α approximates the value of the diffuse attenuation coefficient K_d [1–4, 8–10]. However, at these angles, the information about vertical distribution heterogeneities of the hydrooptical characteristics gets blurred [3]. In [11], several theoretically substantiated sounding procedures are proposed for measuring a set of hydrooptical characteristics, involving changes in the field-of-view angle of the receiving optical system and variations in the sounding angle during measurements, as well as the use of receivers with different directional diagrams. This allows for the estimation of several hydrooptical characteristics but complicates the lidar's design and significantly increases the time required to conduct measurements at each point, which hinders their use in lidar surveys from moving vessels.

Another approach involves using profiling lidars with a "classical" scheme featuring a sufficiently narrow field-of-view angle for the receiving system and establishing regression relationships between the parameters of lidar echo signals and hydrooptical characteristics [5]. The drawback of this method is that the obtained regression relationships are only applicable to the specific sounding scheme used.

In the overwhelming majority of cases, profiling lidars employ a solid-state Nd: YAG laser with frequency conversion to the second harmonic [1]. The radiation from these lasers is linearly polarized. In many lidars, the registration of two mutually orthogonal polarized components of the echo signal is performed — the co-polarized component $P_{co}(t)$ and the cross-polarized component $P_{cross}(t)$. Several studies are dedicated to the processes of forming the polarized components of the echo signal [12–16]. It is proposed to use the depolarization ratio of the lidar echo signal $\delta(t)$, defined as:

$$\delta\left(t=\frac{2z}{c_w}\right)=\frac{P_{cross}(t)}{P_{co}(t)}, \tag{1}$$

a parameter characterizing waters with different hydrooptical characteristics [17, 18]. Here, t is the time measured from the moment the sounding pulse intersects the water surface, and c_w is the speed of light in seawater. In papers [19, 20], an approach is proposed for solving the inverse problem of retrieving the scattering coefficient $b(z)$, based on the use of information about the depth dependence of the degree of depolarization of the echo signal, defined as

$$g\left(t=\frac{2z}{c_w}\right)=\frac{P_{co}(t)-P_{cross}(t)}{P_{co}(t)+P_{cross}(t)}. \tag{2}$$

The difficulty in the practical application of this expression is related to the need for *a priori* information about the values of the depolarization factor ϕ, which cannot be obtained within the lidar sounding.

In works [3–5, 8, 9], regression relations have been found between the parameters of lidar echo signals and hydrooptical characteristics for the co-polarized component of the echo signal, or without considering the polarization of the received radiation. An interesting aspect is finding such regression relations for both orthogonally polarized components of the echo signal and identifying possible features introduced by considering polarization.

The aim of this work is to determine the relationships between a range of hydrooptical characteristics that vary over a wide extent and the parameters of the polarized components of lidar echo signals for a shipborne lidar with a relatively narrow field of view.

2. Materials and methods

2.1. Description of the Equipment

For the research, the marine polarization lidar PLD-1 (developed at SIO RAS [20]) was used. The lidar's dual-channel receiving system is designed to record co- and cross-polarized components of the echo signal. Polarization selection is carried out by film polarizers installed in front of the lenses. The main technical characteristics of the lidar are given in Table 1.

Height of the lidar optical unit above the water surface was approximately 15 m. The sounding angle φ was 20º from the vertical. The length of the air section of the sounding path H was approximately 16 m.

The lidar survey was accompanied by a series of synchronous *in situ* measurements. At each station, vertical profiles of the seawater beam attenuation coefficient c at a wavelength of $\lambda = 530$ nm, seawater temperature, and chlorophyll "a" fluorescence intensity were recorded using a submersible transmissometer PUM-200 (developed at SIO RAS [21]). The accuracy of the seawater beam attenuation coefficient in the range of 0.050–1.0 m^{-1} is 0.005 m^{-1}.

Measurements of the light absorption spectra of seawater $a(\lambda)$ were conducted using a portable spectrophotometer with an integrating sphere (ICAM) [22]. Measurements were carried out on samples collected at the stations, and data processing was performed according to the methodology [23]. The accuracy of the absorption coefficient measurement was 0.05 m^{-1}. The measured set of seawater beam attenuation coefficient and absorption coefficient values at a wavelength of 530 nm enabled the calculation of the single scattering albedo $\omega_0 = b/c$, where the scattering coefficient was determined as $b = c - a$. The difference between the measured values of hydrooptical characteristics at wavelengths $\lambda = 530$ nm and $\lambda = 532$ nm is small compared to the measurement error and can be neglected. For simplicity, the value of the wavelength in the corresponding hydrooptical characteristics is omitted in the following text.

Table 1

Main technical characteristics of PLD-1 lidar

Characteristic	Value
Wavelength of the sounding radiation, nm	532
Duration of the sounding pulse, ns	7
Energy of the sounding pulse, mJ	20
Sounding frequency, Hz	1
Beam divergence of the sounding pulse, mrad	5
Type of polarization of the sounding radiation	Linear
Field of view angle of the receiving optical system of the co-polarized channel, deg. (mrad)	2 (35)
Diameter of the input lens of the co-polarized channel, mm	63
Field of view angle of the receiving optical system of the cross-polarized channel, deg. (mrad)	2 (35)
Diameter of the input lens of the cross-polarized channel, mm	100
Duration of the pulsed characteristic of the lidar, ns	10.8
ADC resolution, bits	14
Digitizing frequency of lidar echo signals, GHz	2.5

At stations conducted during daylight hours, measurements of the vertical profiles of downwelling spectral irradiance $E_d(z, \lambda)$ were performed. The measurements were carried out using a submersible hyperspectral radiometer Ramses (Trios, Germany). The relative error in the measurement of $E_d(z, \lambda)$ is about 8 %. These measurements were used to calculate the diffuse attenuation coefficient K_d of the downwelling solar radiation flux at a wavelength of $\lambda = 532$ nm. At most stations used in this study, underwater irradiance measurements were performed at an average solar zenith angle of 70° under variable cloud conditions. For comparative analysis with lidar estimates, the measured values of K_d were recalculated for the case of direct solar radiation when the sun is at the zenith [10].

2.2. Research area

The studies were conducted within the first stage of the 89th cruise of the R/V "Akademik Mstislav Keldysh" in the western part of the Kara Sea from September 5 to 19, 2022 [24]. Several results of the hydrooptical measurements performed during this cruise are presented in [6, 25]. The hydrooptical characteristics in the study area varied widely: the seawater beam attenuation coefficient c ranged from 0.17 m^{-1} to 1.1 m^{-1}, while the absorption coefficient a ranged from 0.10 m^{-1} to 0.21 m^{-1}.

2.3. Lidar data processing method

This study analyzes the data obtained from lidar sounding conducted at stations with uniform vertical distribution of hydrooptical characteristics within the near-surface layer (0–10 m). The appearance of co- and cross-polarized components of lidar echo signals, recorded in waters of varying transparency, is presented in Fig. 1. In both cases, the decay of the cross-polarized component is more gradual compared to the co-polarized component. This phenomenon is particularly pronounced in turbid waters. The form of the decline of the lidar echo signal in waters homogeneous with depth is determined by two processes: the attenuation of the sounding radiation during its propagation from the surface to a given depth and back to the surface, which is influenced by absorption and scattering, and the process of radiation depolarization, which causes light to transition from one polarized component to another during scattering. Depolarization of light within the water column occurs during single scattering on nonspherical particles and multiple scattering events. The effect of attenuation in the water column is the same for both orthogonally polarized components. However, the effect of the depolarization process on the initial segments of the sounding path is significantly different. This difference is caused by the varying amplitudes of co- and cross-polarized components of the echo signal. In clear waters, the degree of depolarization of the echo signal $g(t)$ at depths of 20–30 meters is 0.8–0.9 [19]. Therefore, in the first approximation, the depolarization process in forming the initial segment of the co-polarized component's decline can be neglected, and an approximation function whose form follows from the lidar equation can be used to describe its shape.

In the quasi-single-scattering approximation, the lidar equation is given as [10, 26]:

$$P\left(t = \frac{2Z}{c_w}\right) = \frac{c_w W_0 S T_O (1-r)^2}{2(nH + Z)^2} \beta'(\pi) \exp\left(-2\alpha Z\right), \tag{3}$$

where Z and H are the lengths of the underwater and above-water portions of the sounding path, c_w is the speed of light in seawater, n is the refractive index of seawater, W_0 is the energy of the sounding pulse, S is the area of the receiving aperture, T_O is the transmittance of the receiving system, $r \approx 0.02$ is the Fresnel reflection coefficient for the air-sea interface, α is the lidar attenuation coefficient, $\beta'(\pi)$ is the effective value of the volume scattering function (VSF) $\beta(\theta)$ at the scattering angle $\theta = 180°$. The true depth z can be recalculated from Z considering the sounding angle φ. The time moment t is measured from the moment the sounding pulse intersects the water surface.

It should be emphasized that in the presented form, the lidar equation can be written only for vertically homogeneous distributions of hydrooptical characteristics. In the case of stratification, α and $\beta'(\pi)$ depend on depth. The approach used in this study, where the decay shape of the lidar echo signal is characterized by a single value of α, becomes inapplicable. The corresponding approximating functions take the form:

$$P_{co}\left(t=\frac{2Z}{c_w}\right)=\frac{A}{(nH+Z)^2}\exp\left(-2\alpha_{co}Z\right), \tag{4}$$

where α_{co} is the lidar attenuation coefficient of the co-polarized component of the echo signal, and A is the approximation coefficient that does not depend on depth.

In the initial segments of the cross-polarized component's decay, the depolarization process plays a significant role. As a result, the lidar equation (3) cannot be directly applied to describe this portion of the signal. However, analysis of extensive experimental data collected during the study indicates that, for these short initial segments, approximating functions $P_{\text{cross}}(t)$ using the lidar attenuation coefficient α_{cross} provide an accurate description of the cross-polarized component's decay.

$$P_{\text{cross}}\left(t=\frac{2Z}{c_w}\right)=\frac{B}{(nH+Z)^2}\exp\left(-2\alpha_{\text{cross}}Z\right), \tag{5}$$

where α_{cross} is the attenuation coefficient of the co-polarized component of the echo signal, and B is the approximation coefficient that does not depend on depth.

In Fig. 1, the dashed lines represent the approximating functions of types (4) and (5). These approximating functions accurately describe the decay shape of the polarized components of the echo signal and allow determining the values of α_{co} and α_{cross}, which characterize the decay rate. To determine α using approximation methods, the decay segment of the echo signal corresponding to a depth range of 4 to 8 meters was used. The echo signal shape above 4 meters is significantly influenced by surface wave activity. Below 8–10 meters, variability in hydrooptical characteristics is often observed, which is associated with stratification.

When processing lidar survey data, the α value was determined for each registered echo signal. Averaging of all obtained α values (from 3,000 to 11,000 soundings) was conducted at stations where the survey duration ranged from 1 to 3 hours, which reduced the influence of random measurement errors. The invariability of hydrooptical characteristics at the station was monitored through the shape of the lidar echo signal and the absence of significant variability in α over time.

The values of α_{co} and α_{cross} thus obtained were used to construct regression relationships of these quantities with various hydrooptical characteristics.

3. Results and discussion

Lidar sounding was aimed at determining the attenuation coefficients of co- and cross-polarized components of the lidar echo signal was conducted at 23 stations, characterized by a homogeneous distribution

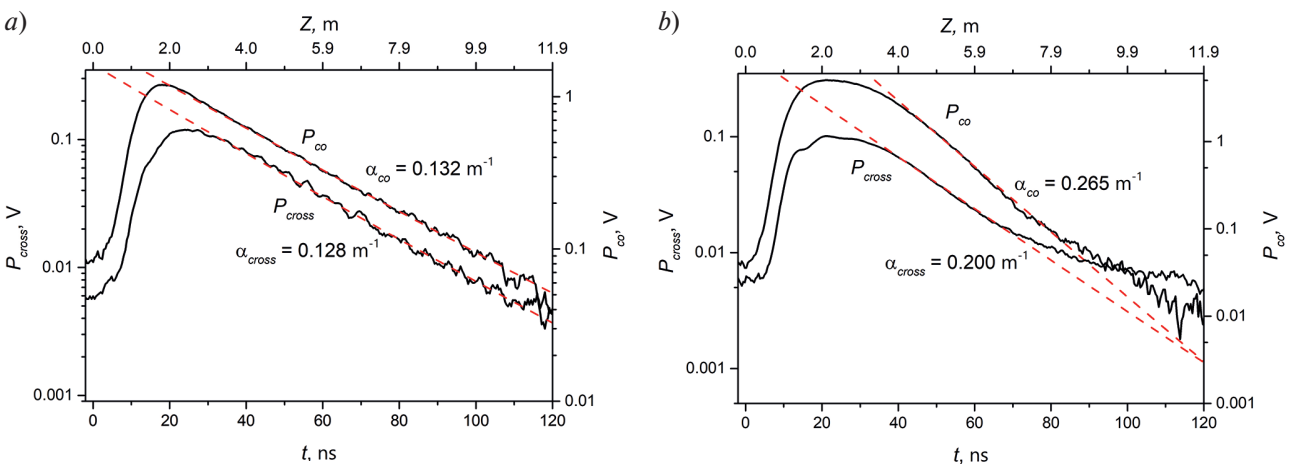

Fig. 1. The examples of co- and cross-polarized components of the echo signal recorded in waters with varying transparency and the corresponding approximation functions: *a* — $c = 0.17$ m^{-1}, *b* — $c = 1.1$ m^{-1}

of hydrooptical characteristics to a depth of 0–10 m. The seawater beam attenuation coefficient ranged from 0.17 m^{-1} to 1.1 m^{-1}, the absorption coefficient a ranged from 0.10 m^{-1} to 0.21 m^{-1}, and the single scattering albedo ω_0 varied from 0.38 to 0.84.

In the case of clear waters (Fig. 1a), characterized by $c = 0.17$ m^{-1}, the values of α_{co} and α_{cross} are close to each other, indicating a relatively small contribution of the depolarization process to the formation of the polarized components. As the scattering coefficient b increases, the differences in the decay forms of the echo signals become more pronounced. For the case of turbid waters, characterized by $c = 1.1$ m^{-1}, the values of α_{co} and α_{cross} differ significantly (Fig. 1b). The decay of the cross-polarized component of the echo signal is more gradual, which suggests a substantial contribution of the depolarization process to the formation of the polarized components of the echo signals. The relationship of the ratio $\alpha_{co}/\alpha_{cross}$ to c is presented in Fig. 2. The colors of the points denote the values of ω_0. A dashed line indicates the linear approximation of the obtained data with a coefficient of determination $R^2 = 0.78$. A comparison of c and ω_0 shows that the increase in the seawater beam attenuation coefficient c is primarily determined by the increase in the scattering coefficient b. This increase leads to a greater contribution of multiple scattering and, consequently, of the depolarization process in the formation of the cross-polarized component of the echo signal. As shown in the graph presented in Fig. 2, the ratio $\alpha_{co}/\alpha_{cross}$ monotonically increases with c and reaches values of 1.3–1.4 in relatively turbid waters.

The obtained dataset allowed for the construction of correlation diagrams that depict the values of α_{co}, α_{cross}, and the hydrooptical characteristics measured concurrently with the lidar sounding. Fig. 3 presents the correlation diagrams for the values of α_{co}, α_{cross} and c. The approximation functions are shown with solid lines, while the dashed lines represent the 95 % confidence intervals. The figure demonstrates the existence of a linear relationship between the lidar attenuation coefficient of the co-polarized component of the echo signal and the seawater beam attenuation coefficient c, with a coefficient of determination $R^2 = 0.95$. For the cross-polarized component, deviations from linear approximation are observed at values of $c > 0.8$ m^{-1} (the R^2 of the linear approximation across the entire dataset is 0.75). The deviation is particularly pronounced when ($c > 1.0$ m^{-1}). This may be related to the increased contribution of the depolarization process in the formation of the cross-polarized component. The magnitude of this contribution is determined by multiple scattering, primarily the second-order scattering, the probability of which is proportional to b^2 [27]. Utilizing a second-degree polynomial as the approximation function provides a significantly better description of the dependence of α_{cross} on c (with $R^2 = 0.88$). Further investigation is needed to understand the relationship between the processes of attenuation and depolarization in the formation of the cross-polarized component of the echo signal.

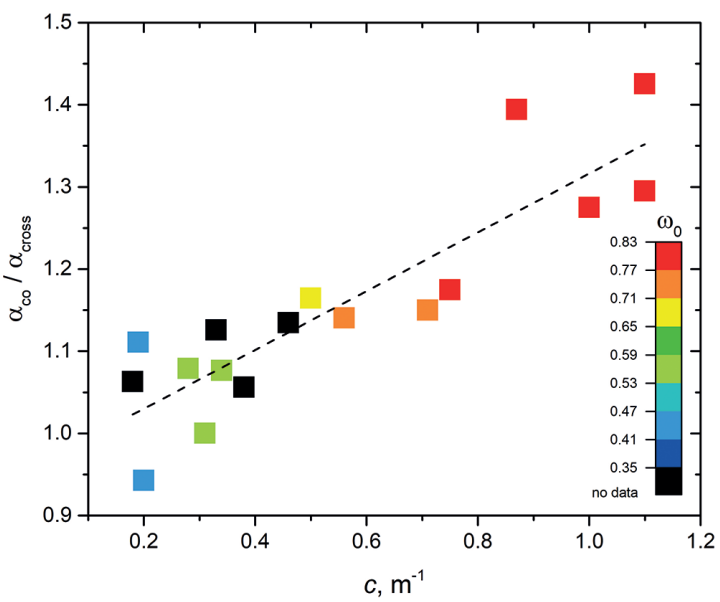

Fig. 2. The relationship between the ratio $\alpha_{co}/\alpha_{cross}$ and c. The color of the points indicates the values of ω_0

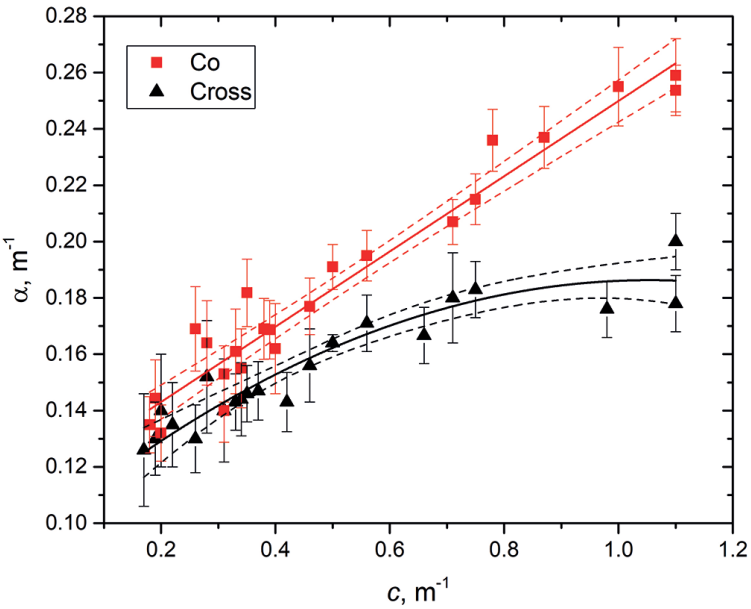

Fig. 3. Correspondence diagram of α_{co}, α_{cross} and c. Approximation functions are shown with solid lines, and 95 % confidence intervals are indicated by dashed lines

Based on the functional dependencies presented in Fig. 3, regression equations have been calculated for the co- and cross-polarized components, allowing the determination of the attenuation coefficient from the values of α_{co} and α_{cross}. These equations are as follows:

$$c_L^{co} = 7.10 \cdot \alpha_{co} - 0.81, \tag{6}$$

$$c_L^{cross} = 62.71 \cdot \alpha_{cross}^2 - 6.93 \cdot \alpha_{cross} + 0.034, \tag{7}$$

where c_L — is the seawater beam attenuation coefficient calculated based on lidar sounding data. The accuracy of regression coefficient determination using the least squares method for co-polarization is 7.10 ± 0.37 and 0.81 m^{-1} ± 0.07 m^{-1}. For cross-polarization, the accuracy is 62.71 m ± 3.34 m, 6.93 ± 0.63, and 0.034 m^{-1} ± ± 0,001 m^{-1}. The relative error in determining c based on lidar sounding data is 10 % for the co-polarized component and 12 % for the cross-polarized component. The derived regression dependencies are valid for seawater beam attenuation coefficient values ranging from 0.17 m^{-1} до 1.1 m^{-1}.

The correspondence diagrams of α_{co}, α_{cross} and the absorption coefficient a are presented in Fig. 4. The figure demonstrates a linear relationship between α_{co} and a ($R^2 = 0.95$) and α_{cross} and a ($R^2 = 0.88$).

The regression equations for the co- and cross-polarized components, which allow for the determination of the absorption coefficient a based on the values of α_{co} and α_{cross}, are as follows:

$$a_L^{co} = 0.74 \cdot \alpha_{co} + 0.008, \tag{8}$$

$$a_L^{cross} = 1.28 \cdot \alpha_{cross} - 0.06, \tag{9}$$

where a_L is the absorption coefficient calculated from lidar sounding data. The accuracy of the regression coefficients estimated using the least squares method for co-polarization is 0.74 ± 0.05 and 0.008 m^{-1} ± 0.001 m^{-1}, while for cross-polarization it is 1.28 ± 0.14 and 0.06 m^{-1} ± 0.01 m^{-1}. The relative error in determining the absorption coefficient a from lidar sounding data for the co-polarized component is 10 %, and for the cross-polarized component it is 12 %.

The diagrams illustrating the correspondence of the values α_{co}, α_{cross}, and the values of the diffuse attenuation coefficient K_d are presented in Fig. 5. The figure demonstrates a linear relationship between α_{co} and K_d ($R^2 = 0.87$) and between α_{cross} and K_d ($R^2 = 0.80$).

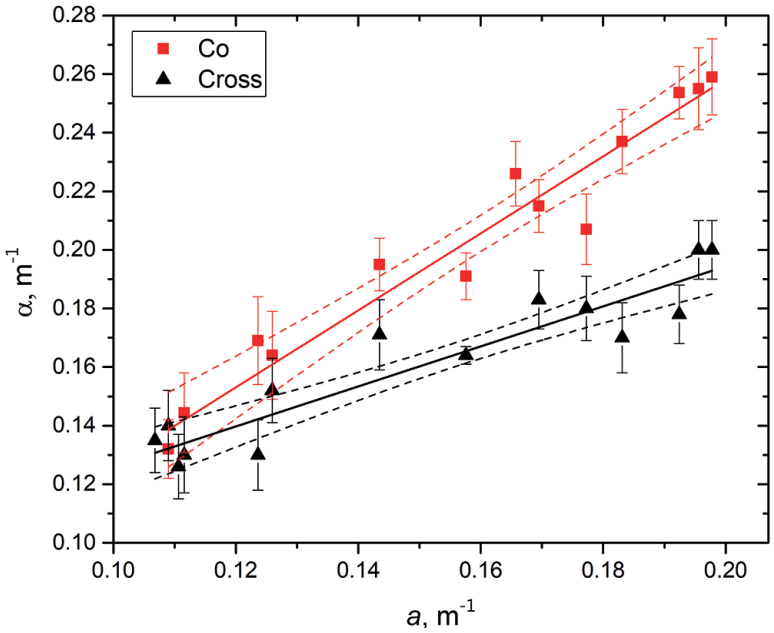

Fig. 4. Correspondence diagram of α_{co}, α_{cross} and a. Approximation functions are shown with solid lines, and 95 % confidence intervals are indicated by dashed lines

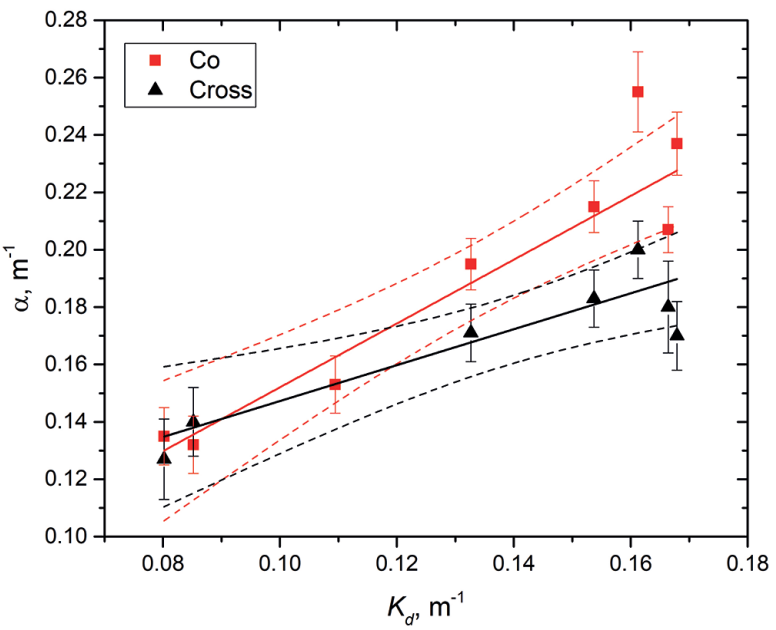

Fig. 5. Correspondence diagram of α_{co}, α_{cross} and K_d. Approximation functions are shown with solid lines, and 95 % confidence intervals are indicated by dashed lines

The regression equations for the co- and cross-polarized components, which allow for the determination of the diffuse attenuation coefficient K_d based on the values of α_{co} and α_{cross}, are as follows:

$$K_{d,L}^{co} = 0.74 \cdot \alpha_{co} - 0.08, \quad (10)$$

$$K_{d,L}^{cross} = 1.34 \cdot \alpha_{cross} - 0.09, \quad (11)$$

where $K_{d,L}$ is the diffuse attenuation coefficient calculated from lidar sounding data. The accuracy of the regression coefficients for co-polarization is 0.74 ± 0.11 and 0.08 m^{-1} ± 0.01 m^{-1}, while for cross-polarization it is 13.05 ± 1.22 and 1.53 m^{-1} ± 0.19 m^{-1}. The relative error in determining $K_{d,L}$ from lidar sounding data for the co-polarized component is 12 %, and for the cross-polarized component, it is 13 %.

The obtained regression relations for α_{co}, α_{cross}, and a set of hydrooptical characteristics are valid for lidars with the beam divergence and field of view angle of the receiving optical system indicated in Table 1, as well as for the sounding geometry described in Section 2.1. In the case of changes in the sounding geometry and lidar characteristics (primarily the field of view angle of the receiving system), adjustments to the regression coefficient relationships will be required.

4. Conclusion

Lidar sounding conducted at stations with a homogeneous vertical distribution of hydrooptical characteristics in the near-surface layer, along with synchronous contact measurements of various hydrooptical characteristics, resulted in a large dataset. The studies were conducted in the western part of the Kara Sea. Statistical processing of these data allowed for the establishment of regression relationships linking c, a, K_d to the lidar attenuation coefficients of the co- and cross-polarized components of the lidar echo signal. The regression relationships enable the use of lidar survey data taken on board a moving vessel to assess the spatial distributions of hydrooptical characteristics necessary for solving various practical tasks.

The data obtained using the cross-polarized component of the lidar echo signal largely replicate the data from the co-polarized component. However, using a dual-channel recording system enhances the reliability and accuracy of the obtained data. Furthermore, the registration of two orthogonally polarized components of the lidar echo signal allows for the calculation of depth-dependent depolarization ratios $\delta(z)$, which are sensitive to various vertical inhomogeneities within the water column. This enables the use of lidar survey data for monitoring the uniformity of the vertical distribution of hydrooptical characteristics in the near-surface layer of seawater and for filtering measurement data in stratified waters [15–17].

Future research efforts will focus on conducting studies in different marine areas of the World Ocean, characterized by varying values of hydrooptical characteristics, as well as distinct sounding geometries and field of view angles of the receiving optical system. The resulting data will be useful for the necessary adjustments to be made to the regression relationships.

Acknowledgments

The authors gratefully acknowledge V.A. Artemyev, M.A. Pavlova, S.K. Klimenko and D.N. Deryagin for assistance in carrying out contact measurements.

Funding

The processing and statistical analysis of the recorded lidar sounding data were carried out within the Shirshov Institute of Oceanology state assignment (No. FMWE-2024–0015). The processing of related data was sponsored under the project funded by the Russian Hydrometeorological Service (contract agreement No. 169-15-2023-002).

References

1. Glukhov V.A., Goldin Yu.A. Marine profiling lidars and their application for oceanological problems. *Fundamental and Applied Hydrophysics*. 2024;17(1):104–128. doi:10.59887/2073–6673.2024.17(1)-9
2. Bravo-Zhivotovsky D.M., Gordeev L.B., Dolin L.S., Mochenev S.B. Determination of absorption and scattering indicators of sea water based on some characteristics of the light field of artificial light sources. *Hydrophysical and hydrooptical studies in the Atlantic and Pacific oceans. Based on the results of research on the 5th cruse of the R/V Dmitry Mendeleev. Chapter 5*. Pp. 153–158 / Ed. by A.S. Monin, K.S. Shifrin. M.: Nauka; 1974. 328 p. (in Russian).
3. Peituo Xu, Dong Liu, Yibing Shen et al. Design and validation of a shipborne multiple-field-of-view lidar for upper ocean remote sensing. *Journal of Quantitative Spectroscopy and Radiative Transfer*. 2020;254:107201. doi:10.1016/j.jqsrt.2020.107201

4. Collister B.L., Zimmerman R.C., Hill V.J., Sukenik I., Balch M. Polarized lidar and ocean particles: insights from a mesoscale coccolithophore bloom. *Applied Optics*. 2020;59(15):4650–4662. doi:10.1364/AO.389845
5. Glukhov V.A., Goldin Yu.A., Glitko O.V. et al. Investigation of the Relationships between the Parameters of Lidar Echo Signals and Hydrooptical Characteristics in the Western Kara Sea. *Oceanology*. 2023;63(Suppl 1): S119-S130. doi:10.1134/S0001437023070044
6. Glukhov V.A., Goldin Yu.A., Glitko O.V. et al. Lidar Research during the First Stage of the 89th Cruise of the R/V "Academic Mstislav Keldysh". *Fundamental and Applied Hydrophysics*. 2023;16(4):107–115. doi:10.59887/2073-6673.2023.16(4)-9
7. Chen Ya., Cui X., Gu Q. et al. This is MATE: A Multiple scAttering correcTion rEtrieval algorithm for accurate lidar profiling of seawater optical properties. *Remote Sensing of Environment*. 2024;307:114166. doi:10.1016/j.rse.2024.114166
8. Zhou Y., Chen Y., Zhao H. et al. Shipborne oceanic high-spectral-resolution lidar for accurate estimation of seawater depth-resolved optical properties. *Light: Science & Applications*. 2022;11:261. doi:10.1038/s41377-022-00951-0
9. Schulien J.A., Behrenfeld M.J., Hair J.W. et al. Vertically- resolved phytoplankton carbon and net primary production from a high spectral resolution lidar. *Optic Express*. 2017;25:13577–13587. doi:10.1364/OE.25.013577
10. Gordon H.R. Interpretation of airborne oceanic lidar: effects of multiple scattering. *Applied Optics*. 1982;21(16): 2996–3001.
11. Dolina I.S., Dolin L.S., Levin I.M., Rodionov A.A., Savel'ev V.A. Inverse problems of lidar sensing of the ocean. *Current Research on Remote Sensing, Laser Probing, and Imagery in Natural Waters. SPIE*. 2007;6615:104–113.
12. Chaikovskaya L.I., Zege E.P. Theory of polarized lidar sounding including multiple scattering. *Journal of Quantitative Spectroscopy and Radiative Transfer*. 2004;88(1–3):21–35. doi:10.1016/j.jqsrt.2004.01.002
13. Vasilkov A.P., Kondranin T.V., Myasnikov E.V. Determination of the light scattering index profile based on the polarization characteristics of back-reflected radiation during pulsed ocean sounding. *Izvestiya AS USSR, Atmospheric and Ocean Physics*. 1990;26(3):307–312 (in Russian).
14. Goldin Yu.A., Rogozkin D.B., Sheberstov S.V. Polarized Lidar Sounding of Stratified Seawater. *Proceedings of IV International Conference "Current Problems in Optics of Natural Waters (ONW'2007)"*. Nizhny Novgorod; 2007. P. 175–178.
15. Krekov G.M., Krekova M.M., Shamanaev V.S. Laser sensing of a subsurface oceanic layer. II. Polarization characteristics of signals. *Applied Optics*. 1998;37:1596–1601. doi:10.1364/AO.37.001596
16. Churnside J.H. Polarization effects on oceanographic lidar. *Optics express*. 2008;16(2):1196–1207. doi:10.1364/OE.16.001196
17. Kokhanenko G.P., Balin Y.S., Penner I.E., Shamanaev V.S. Lidar and in situ measurements of the optical parameters of water surface layers in Lake Baikal. *Atmospheric and Oceanic Optics*. 2011;24(5):478–486. doi:10.1134/S1024856011050083
18. Churnside J.H. Review of profiling oceanographic lidar. *Optical Engineering*. 2014;53(5):051405–051405. doi:10.1117/1.OE.53.5.051405
19. Vasilkov A.P., Goldin Yu.A., Gureev B.A., Hoge F.E., Swift R.N., Wright C.W. Airborne polarized lidar detection of scattering layers in the ocean. *Applied Optics*. 2001;40(24):4353–4364. doi:10.1364/AO.40.004353
20. Glukhov V.A., Goldin Yu.A., Rodionov M.A. Experimental estimation of the capabilities of the lidar PLD-1 for the registration of various hydro-optical irregularities of the sea water column. *Fundamental and Applied Hydrophysics*. 2017;10(2):41–48 doi:10.7868/S207366731702006X (in Russian).
21. Artemiev V.A., Taskaev V.R., Grigoriev A.V. Autonomous transparent meter PUM-200. *Materials of the XVII International Scientific and Technical Conference (MSOI-2021)*, Moscow: 2021. P. 95–99 (in Russian).
22. Pogosyan S.I., Durgaryan A.M., Konyukhov I.V. et al. Absorption spectroscopy of microalgae, cyanobacteria, and dissolved organic matter: Measurements in an integrating sphere cavity. *Oceanology*. 2009;49:866–871. doi:10.1134/S0001437009060125
23. Glukhovets D.I., Sheberstov S.V., Kopelevich O.V. et al. Measuring the sea water absorption factor using integrating sphere. *Light & Engineering*. 2018;26(1):120–126.
24. Kravchishina M.D., Klyuvitkin A.A., Novigatskiy A.N. et al. The 89th cruise (1st stage) of the research vessel "Academician Mstislav Keldysh": climatic experiment in interaction with the Tu-134 "Optik" laboratory aircraft in the Kara Sea. *Oceanology*. 2023;63(3):1–4. doi:10.31857/S0030157423030073
25. Glukhovets D.I., Aglova E.A., Artemiev V.A. et al. Results of Hydrooptical Field Studies in the Barents and Kara Seas in September 2022. *Complex Investigation of the World Ocean (CIWO-2023). Springer Proceedings in Earth and Environmental Sciences*. Cham: Springer; 2023. P. 439–445. doi:10.1007/978-3-031-47851-2_53
26. Dolin L.S., Savelev V.A. Characteristics of the backscattering signal during pulsed irradiation of a turbid medium by a narrow directed light beam. *Izvestiya AS USSR, Atmospheric and Ocean Physics*. 1971;7:505–510 (in Russian).
27. Ernst A. *Multiple-scattering theory. New developments and applications*. Halle-Wittenberg University: 2007. 65 p.

Литература

1. *Глухов В.А., Гольдин Ю.А.* Морские радиометрические лидары и их использование для решения океанологических задач // Фундаментальная и прикладная гидрофизика. 2024. Т. 17, № 1. С. 104–128. doi:10.59887/2073-6673.2024.17(1)-9
2. *Браво-Животовский Д.М., Гордеев Л.Б., Долин Л.С., Моченев С.Б.* Определение показателей поглощения и рассеяния морской воды по некоторым характеристикам светового поля искусственных источников света // Гидрофизические и гидрооптические исследования в Атлантическом и Тихом океанах. По результатам исследований в 5-м рейсе НИС «Дмитрий Менделеев». Глава 5. С. 153–158 / Под ред. А.С. Монина, К.С. Шифрина. М.: Наука, 1974. 328 с.
3. *Xu P., Liu D., Shen Y., Chen Y.* Design and validation of a shipborne multiple-field-of-view lidar for upper ocean remote sensing // Journal of Quantitative Spectroscopy and Radiative Transfer. 2020. Vol. 254. P. 107201. doi:10.1016/j.jqsrt.2020.107201
4. *Collister B.L., Zimmerman R.C., Hill V.J., Sukenik I., Balch M.* Polarized lidar and ocean particles: insights from a mesoscale coccolithophore bloom // Applied Optics. 2020. Vol. 59, № 15. P. 4650–4662. doi:10.1364/AO.389845
5. *Glukhov V.A., Goldin Yu.A., Glitko O.V.* et al. Investigation of the Relationships between the Parameters of Lidar Echo Signals and Hydrooptical Characteristics in the Western Kara Sea // Oceanology. 2023. Vol. 63 (S1). P. S119–S130. doi:10.1134/S0001437023070044
6. *Глухов В.А., Гольдин Ю.А., Глитко О.В., Аглова Е.А., Глуховец Д.И., Родионов М.А.* Лидарные исследования в первом этапе 89-го рейса НИС «Академик Мстислав Келдыш» // Фундаментальная и прикладная гидрофизика. 2023. Т. 16. № 4. С. 107–115. doi:10.59887/2073–6673.2023.16(4)-9
7. *Chen Ya., Cui X., Gu Q.* et al. This is MATE: A Multiple scAttering correcTion rEtrieval algorithm for accurate lidar profiling of seawater optical properties // Remote Sensing of Environment. 2024. Vol. 307. P. 114166. doi:10.1016/j.rse.2024.114166
8. *Zhou Y., Chen Y., Zhao H.* et al. Shipborne oceanic high-spectral-resolution lidar for accurate estimation of seawater depth-resolved optical properties // Light: Science & Applications. 2022. Vol. 11. P. 261. doi:10.1038/s41377–022-00951-0
9. *Schulien J.A., Behrenfeld M.J., Hair J.W.* et al. Vertically- resolved phytoplankton carbon and net primary production from a high spectral resolution lidar // Optic Express. 2017. Vol. 25. P. 13577–13587. doi:10.1364/OE.25.013577
10. *Gordon H.R.* Interpretation of airborne oceanic lidar: effects of multiple scattering // Applied Optics. 1982. Vol. 21. N16. P. 2996–3001.
11. *Dolina I.S., Dolin L.S., Levin I.M., Rodionov A.A., Savel'ev V.A.* Inverse problems of lidar sensing of the ocean // Current Research on Remote Sensing, Laser Probing, and Imagery in Natural Waters. SPIE. 2007. Vol. 6615. P. 104–113.
12. *Chaikovskaya L.I., Zege E.P.* Theory of polarized lidar sounding including multiple scattering // Journal of Quantitative Spectroscopy and Radiative Transfer. 2004. Vol. 88, N1–3. P. 21–35. doi:10.1016/j.jqsrt.2004.01.002
13. *Васильков А.П., Кондранин Т.В., Мясников Е.В.* Определение профиля показателя рассеяния света по поляризационным характеристикам отраженного назад излучения при импульсном зондировании океана // Известия АН СССР. Физика атмосферы и океана. 1990. Т. 26, № 3. С. 307–312.
14. *Goldin Yu.A., Rogozkin D.B., Sheberstov S.V.* Polarized Lidar Sounding of Stratified Seawater // Proceedings of IV International Conference "Current Problems in Optics of Natural Waters (ONW'2007)". Nizhny Novgorod. 2007. P. 175–178.
15. *Krekov G.M., Krekova M.M., Shamanaev V.S.* Laser sensing of a subsurface oceanic layer. II. Polarization characteristics of signals // Applied Optics. 1998. Vol. 37. P. 1596–1601. doi:10.1364/AO.37.001596
16. *Churnside J.H.* Polarization effects on oceanographic lidar // Optics express. 2008. Vol. 16, N 2. P. 1196–1207. doi:10.1364/OE.16.001196
17. *Коханенко Г.П., Балин Ю.С., Пеннер И.Э., Шаманаев В.С.* Лидарные и in situ измерения оптических параметров поверхностных слоев воды в озере Байкал // Оптика атмосферы и океана. 2011. Т. 24, № 5. С. 377–385.
18. *Churnside J.H.* Review of profiling oceanographic lidar // Optical Engineering. 2014. Vol. 53, N 5. P. 051405–051405. doi:10.1117/1.OE.53.5.051405
19. *Vasilkov A. P., Goldin Yu.A., Gureev B.A., Hoge F.E., Swift R.N., Wright C.W.* Airborne polarized lidar detection of scattering layers in the ocean // Applied Optics. 2001. Vol. 40, N. 24. P. 4353–4364. doi:10.1364/AO.40.004353
20. *Глухов В.А., Гольдин Ю.А., Родионов М.А.* Экспериментальная оценка возможностей лидара ПЛД-1 по регистрации гидрооптических неоднородностей в толще морской среды // Фундаментальная и прикладная гидрофизика. 2017. Т. 10, № 2. С. 41–48. doi:10.7868/S207366731702006X

21. *Артемьев В.А., Таскаев В.Р., Григорьев А.В.* Автономный прозрачномер ПУМ-200 // В сборнике: Современные методы и средства океанологических исследований (МСОИ-2021). Материалы XVII международной научно-технической конференции. Институт океанологии им. П.П. Ширшова РАН. 2021. С. 95–99.
22. *Погосян С.И., Дургарян А.М., Конюхов И.В.* и др. Абсорбционная спектроскопия микроводорослей цианобактерий и растворенного органического вещества: измерения во внутренней полости интегрирующей сферы // Океанология. 2009. Т. 49. С. 934–939.
23. *Глуховец Д.И., Шеберстов С.В., Копелевич О.В. и др.,* Измерения показателя поглощения морской воды с помощью интегрирующей сферы // Светотехника. 2017. № 5. С. 39–43.
24. *Кравчишина М.Д, Клювиткин А.А, Новигатский А.Н. и др.* 89-й рейс (1-й этап) научно-исследовательского судна “Академик Мстислав Келдыш”: климатический эксперимент во взаимодействии с самолетом-лабораторией Ту-134 “Оптик” в Карском море // Океанология. 2023. Т. 63, № 3. С. 1–4. doi:10.31857/S0030157423030073
25. *Glukhovets D.I., Aglova E.A., Artemiev V.A. et al.* Results of Hydrooptical Field Studies in the Barents and Kara Seas in September 2022 // Complex Investigation of the World Ocean (CIWO-2023). Springer Proceedings in Earth and Environmental Sciences. Springer, Cham. 2023. P. 439–445. doi:10.1007/978-3-031-47851-2_53
26. *Долин Л.С., Савельев В.А.* О характеристиках сигнала обратного рассеяния при импульсном облучении мутной среды узким направленным световым пучком // Известия АН СССР. Физика атмосферы и океана. 1971. Т. 7, № 5. С. 505–510.
27. *Ernst A.* Multiple-scattering theory. New developments and applications. Halle-Wittenberg University. 2007. 65 c.

About the Authors

GLUKHOV, Vladimir A. Researcher, IO RAS, ORCID: 0000-0003-4555-8879, WoS ResearcherID: GSD-4886–2022, Scopus Author ID: 57191414331, SPIN-code: 9449-2307, e-mail: vl.glukhov@inbox.ru

GOLDIN, Yury A. Cand. Sc. (Phys.-Math.), Leading Researcher, IO RAS, ORCID: 0000-0001-5731-5458, Scopus Author ID: 6602648464, SPIN-code: 2750-1867, e-mail: goldin@ocean.ru

GLITKO, Oleg V. Researcher, IO RAS, ORCID: 0009-0005-2313-2326. e-mail: glitko_kisin@mail.ru

GLUKHOVETS, Dmitry I. Cand. Sc. (Phys.-Math.), Leading Researcher, IO RAS; associate professor Moscow Institute of Physics and Technology (National Research University), ORCID: 0000-0001-5641-4227, Scopus AuthorID: 57193736311, SPIN-code (РИНЦ): 6755-2450, e-mail: glukhovets@ocean.ru

RODIONOV, Maxim A. Cand. Sc. (Phys.-Math.), Leading Researcher, IO RAS, ORCID: 0000-0002-7397-0548, Scopus AuthorID: 56034199200, SPIN-code (РИНЦ): 5706-0570.